Hindawi Publishing Corporation
Advances in High Energy Physics
Volume 2015, Article ID 763648, 17 pages
http://dx.doi.org/10.1155/2015/763648

Research Article

Standard and Nonstandard Neutrino-Nucleus Reactions Cross Sections and Event Rates to Neutrino Detection Experiments

D. K. Papoulias and T. S. Kosmas

Division of Theoretical Physics, University of Ioannina, 45100 Ioannina, Greece

Correspondence should be addressed to D. K. Papoulias; dimpap@cc.uoi.gr

Received 11 July 2014; Accepted 3 November 2014

Academic Editor: Athanasios Hatzikoutelis

In this work, we explore ν-nucleus processes from a nuclear theory point of view and obtain results with high confidence level based on accurate nuclear structure cross sections calculations. Besides cross sections, the present study includes simulated signals expected to be recorded by nuclear detectors and differential event rates as well as total number of events predicted to be measured. Our original cross sections calculations are focused on measurable rates for the standard model process, but we also perform calculations for various channels of the nonstandard neutrino-nucleus reactions and come out with promising results within the current upper limits of the corresponding exotic parameters. We concentrate on the possibility of detecting (i) supernova neutrinos by using massive detectors like those of the GERDA and SuperCDMS dark matter experiments and (ii) laboratory neutrinos produced near the spallation neutron source facilities (at Oak Ridge National Lab) by the COHERENT experiment. Our nuclear calculations take advantage of the relevant experimental sensitivity and employ the severe bounds extracted for the exotic parameters entering the Lagrangians of various particle physics models and specifically those resulting from the charged lepton flavour violating $\mu^- \to e^-$ experiments (Mu2e and COMET experiments).

1. Introduction

Coherent scattering of neutrinos on complex nuclei was proposed long ago [1, 2] as a prominent probe to study neutral-current (NC) ν-nucleus processes, but up to now no events have been experimentally measured. Neutrino detection constitutes an excellent probe to search for a plethora of conventional neutrino physics applications and new-physics open issues [3–5]. In principle, low-energy astrophysical and laboratory neutrino searches provide crucial information towards understanding the underling physics of the fundamental electroweak interactions within and beyond the SM [6, 7]. Well-known neutrino sources include (i) supernova neutrinos (with energies up to 60–100 MeV) and (ii) laboratory neutrinos (with energies up to 52.8 MeV) emerging from stopped-pion and muon decays at muon factories (Fermilab, PSI, JPARC, etc.) and at the spallation neutron source (SNS) at Oak Ridge National Lab [8]. Recently, it became feasible [9] to detect neutrinos by exploiting the neutral current interactions and measuring the nuclear recoil signals through the use of very low threshold-energy detectors [10, 11]. To this purpose, great experimental effort has been put and new experiments have been proposed to be performed at facilities with stopped-pion neutrino beams, based on promising nuclear detectors like those of the COHERENT experiment [12, 13] and others [14] at the SNS, or alternative setups at the Booster Neutrino Beam (BNB) at Fermilab [15, 16]. The nuclear ν-detectors adopted by the relevant experiments include liquid noble gases, such as ^{20}Ne, ^{40}Ar, and ^{132}Xe, as well as ^{76}Ge and CsI[Na] detection materials [17].

On the theoretical side, the ν-signals of low-energy neutrinos, expected to be recorded in sensitive nuclear detectors [18–20], could be simulated through nuclear calculations of ν-nucleus scattering cross sections. Such results may provide useful information relevant for the evolution of distant stars, the core collapse supernovae, explosive nucleosynthesis, and other phenomena [21, 22]. In fact, coherent neutral current ν-nucleus scattering events are expected to be observed by using the high intensity stopped-pion neutrino beams

[23, 24] and nuclear targets for which recoil energies are of the order of a few to tens of keV and therefore appropriate for detection of WIMPs [25, 26], candidates of cold dark matter [27–29]. Such detectors are, for example, the SuperCDMS [30], GERDA [31], and other multipurpose detectors [32–34]. For low energies, the dominant vector components of NC interactions lead to a coherent contribution of all nucleons (actually all neutrons) in the target nucleus [35–37].

It is worth mentioning that, after the discovery [38–42] of neutrino oscillations in propagation, the challenge of neutral and charged lepton flavour violation (LFV) is further investigated by extremely sensitive experiments [43–49] searching for physics beyond the current standard model (SM) [50]. To this end, neutrino-nucleus coherent scattering experiments may probe new physics beyond the SM involved in exotic neutrino-nucleus interactions [9, 51–53], an undoubtable signature of nonstandard physics. Therefore, new data and insights will be provided to the physics of flavour changing neutral-current (FCNC) processes, in the leptonic sector, in nonstandard neutrino oscillation effects [54–56], in neutrino transition magnetic moments [57], in sterile neutrino search [58], and others [59]. Furthermore, such experimental sensitivity may also inspire advantageous probes to shed light on various open issues in nuclear astrophysics [60, 61].

In recent works [53], neutral-current (NC) nonstandard interactions (NSI) involving (anti)neutrino scattering processes on leptons, nucleons, and nuclei have been investigated. The reactions of this type that take place in nuclei are represented by

$$\nu_\alpha\left(\widetilde{\nu}_\alpha\right) + (A, Z) \longrightarrow \nu_\beta\left(\widetilde{\nu}_\beta\right) + (A, Z) \tag{1}$$

($\alpha, \beta = e, \mu, \tau$ with $\alpha \neq \beta$). It has been suggested [62] that, theoretically, the latter processes can be studied with the same nuclear methods as the exotic cLFV process of $\mu^- \rightarrow e^-$ conversion in nuclei [63–66]. The corresponding Lagrangians may be derived within the context of various extensions of the SM [6, 7, 67], like the four-fermion contact interaction, seesaw model [68, 69], left-right symmetric models [70], gluonic operator model [71], and so forth.

It is well known that neutrino NSI may have rather significant impact in many areas of modern physics research and thus motivate a great number of similar studies [72]. Particularly in astrophysical applications, constraints coming out of some supernova explosion scenarios [73–75] may be affected and eventually lead to the necessity of further investigation of NSI in both LFV and cLFV processes that may occur in solar and supernova environment [76–80]. Such open issues motivated our present work too.

One of our main purposes in this paper, which is an extension of our previous study [53], is to comprehensively study the above issues by performing nuclear structure calculations for a set of experimentally interesting nuclei. We estimate reliably the nuclear matrix elements describing both interaction channels, the exotic and the standard model ones, but we mainly focus on the SM component of the neutrino-nucleus processes; that is, we consider $\alpha = \beta$ in the reactions of (1). Exotic neutrino-nucleus events are also computed. By exploiting our accurate original cross sections, we obtain simulated ν-signals and flux averaged cross sections which are experimentally interesting quantities for both supernova and SNS neutrinos. The total number of events expected to be recorded over the energy threshold for the studied nuclear targets is also presented for both cases.

We stress the fact that we have devoted special effort to obtain results of high accuracy by constructing the nuclear ground state within the context of the quasiparticle random phase approximation (QRPA), that is, by solving iteratively the BCS equations for realistic pairing interactions (the Bonn C-D potential) [81–83], and achieving high reproducibility of the available experimental data [84]. In addition, we made comparisons with the results of other methods evaluating the nuclear form factors that enter the coherent rate [85, 86] as the one which employs fractional occupation probabilities (FOP) of the states (on the basis of analytic expressions) [87] and other well-known methods [88].

2. Description of the Formalism

In this section, we present briefly the necessary formalism for describing all channels of the NSI processes of the reactions (1), derived by starting from the corresponding nuclear-level Feynman diagrams.

In Figure 1, the exchange of a Z-boson between a lepton and a nucleon is represented, for the SM ν-nucleus scattering, Figure 1(a), and for the exotic ν-nucleus scattering, Figure 1(b). As already mentioned in the Introduction, the nonstandard ν-nucleus processes [53] and the exotic cLFV $\mu^- \rightarrow e^-$ conversion in nuclei [50, 63, 76, 77, 79, 80] can be predicted within the context of the same new-physics models [62, 68]. For this reason, in Figure 1(c), we also show the exchange of a Z-boson or a virtual γ-photon leading to the nuclear $\mu^- \rightarrow e^-$ conversion [64, 68]. Thus, the leptonic vertex in the cases of Figures 1(b) and 1(c) is a complicated one. A general effective Lagrangian that involves SM interactions ($\mathscr{L}_{\mathrm{SM}}$) and NSI ($\mathscr{L}_{\mathrm{NSI}}$) with a nonstandard flavour preserving (FP) term, a nonuniversal (NU) term, and a flavour changing (FC) term reads

$$\mathscr{L}_{\mathrm{tot}} = \mathscr{L}_{\mathrm{SM}} + \mathscr{L}_{\mathrm{NSI}} = \mathscr{L}_{\mathrm{SM}} + \mathscr{L}_{\mathrm{NU}} + \mathscr{L}_{\mathrm{FC}}. \tag{2}$$

Each of the components $\mathscr{L}_{\mathrm{SM}}$ and $\mathscr{L}_{\mathrm{NSI}}$, the individual terms $\mathscr{L}_{\mathrm{NU}}$ and $\mathscr{L}_{\mathrm{FC}}$, and the nuclear matrix elements that arise from each part are discussed below.

2.1. Coherent Cross Sections of Nonstandard ν-Nucleus Reactions. The quark-level Lagrangian for neutral current nonstandard neutrino interactions $\mathscr{L}_{\mathrm{NSI}}$, at the four-fermion approximation (energies $\ll M_Z$), is parametrized as [9, 52, 73]

$$\mathscr{L}_{\mathrm{NSI}} = -2\sqrt{2}G_F \sum_{\substack{f=u,d \\ \alpha,\beta=e,\mu,\tau}} \epsilon_{\alpha\beta}^{fP}\left[\overline{\nu}_\alpha\gamma_\rho L\nu_\beta\right]\left[\overline{f}\gamma^\rho Pf\right], \tag{3}$$

where f denotes a first generation SM quark, ν_α are three light neutrinos with Majorana masses, and $P = \{L, R\}$ are the chiral projectors. In the latter Lagrangian (3), two classes of

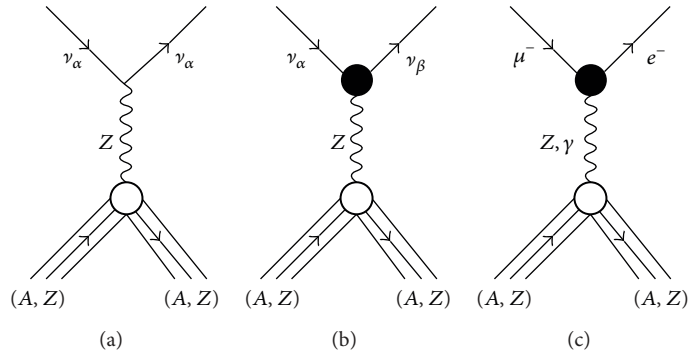

FIGURE 1: Nuclear level Feynman diagrams for (a) SM Z-exchange neutral-current ν-nucleus reactions, (b) nonstandard Z-exchange ν-nucleus reactions, and (c) Z-exchange and photon-exchange $\mu^- \to e^-$ in the presence of a nucleus (muon-to-electron conversion). The nonstandard (cLFV or LFV) physics enters in the complicated vertex denoted by the bullet • [53].

nonstandard terms are considered (i) flavour preserving non-SM terms that are proportional to $\epsilon_{\alpha\alpha}^{fP}$ (known as nonuniversal, NU interactions) and (ii) flavour changing (FC) terms proportional to $\epsilon_{\alpha\beta}^{fP}$, $\alpha \neq \beta$. These couplings are defined with respect to the strength of the Fermi coupling constant G_F [52, 73]. In the present work, we examine spin-zero nuclei; thus, the polar-vector couplings defined as $\epsilon_{\alpha\beta}^{fV} = \epsilon_{\alpha\beta}^{fL} + \epsilon_{\alpha\beta}^{fR}$ are mainly of interest. For the axial-vector couplings it holds $\epsilon_{\alpha\beta}^{fA} = \epsilon_{\alpha\beta}^{fL} - \epsilon_{\alpha\beta}^{fR}$.

Following [79, 80], the nuclear physics aspects of the neutrino-matter NSI can be explored by transforming the quark-level Lagrangian (3) eventually to the nuclear level where the hadronic current is written in terms of NC nucleon form factors that are functions of the four-momentum transfer. Generally, for inelastic ν-nucleus scattering, the magnitude of the three-momentum transfer, $q = |\vec{q}|$, is a function of the scattering angle of the outgoing neutrino θ (in laboratory frame) and the initial, E_i, and final, E_f, nuclear energies, as well as the excitation energy of the target nucleus, ω, and takes the form $q^2 = \omega^2 + 2E_iE_f(1 - \cos\theta)$ [81, 85]. Our analysis in the present paper concentrates on the dominant coherent (elastic) channel where only $gs \to gs$ transitions occur ($\omega = 0$, $E_i = E_f$) and the momentum transfer in terms of the incoming neutrino energy, E_ν, becomes $q^2 = 2E_\nu^2(1 - \cos\theta)$ or equivalently $q = 2E_\nu \sin(\theta/2)$.

The NSI coherent differential cross section of neutrinos scattering off a spin-zero nucleus, with respect to the scattering angle θ, reads [53]

$$\frac{d\sigma_{\mathrm{NSI},\nu_\alpha}}{d\cos\theta} = \frac{G_F^2}{2\pi}E_\nu^2(1 + \cos\theta)\left|\langle gs|\left|G_{V,\nu_\alpha}^{\mathrm{NSI}}(q)\right||gs\rangle\right|^2, \quad (4)$$

where $\alpha = e, \mu, \tau$ denotes the flavour of incident neutrinos and $|gs\rangle$ represents the nuclear ground state (for even-even nuclei assumed here, $|gs\rangle = |J^\pi\rangle \equiv |0^+\rangle$). The nuclear matrix element, which enters the cross section of (4), is written as [53]

$$\begin{aligned}&\left|\mathscr{M}_{V,\nu_\alpha}^{\mathrm{NSI}}\right|^2 \\ &\equiv \left|\langle gs|\left|G_{V,\nu_\alpha}^{\mathrm{NSI}}(q)\right||gs\rangle\right|^2 \\ &= \left[\left(2\epsilon_{\alpha\alpha}^{uV} + \epsilon_{\alpha\alpha}^{dV}\right)ZF_Z\left(q^2\right) + \left(\epsilon_{\alpha\alpha}^{uV} + 2\epsilon_{\alpha\alpha}^{dV}\right)NF_N\left(q^2\right)\right]^2 \\ &\quad + \sum_{\beta\neq\alpha}\left[\left(2\epsilon_{\alpha\beta}^{uV} + \epsilon_{\alpha\beta}^{dV}\right)ZF_Z\left(q^2\right) + \left(\epsilon_{\alpha\beta}^{uV} + 2\epsilon_{\alpha\beta}^{dV}\right)NF_N\left(q^2\right)\right]^2\end{aligned} \quad (5)$$

($\beta = e, \mu, \tau$) where $F_{Z(N)}$ denote the nuclear (electromagnetic) form factors for protons (neutrons). We stress the fact that, in the adopted NSI model, the coherent NC ν-nucleus cross section is not flavour blind as in the SM case. Obviously, by incorporating the nuclear structure details, in (4) and (5), the cross sections become more realistic and accurate [9]. The structure of the Lagrangian (2) implies that in the right-hand side of (5) the first term is the NU matrix element, $\mathscr{M}_{V,\nu_\alpha}^{\mathrm{NU}}$, and the summation is the FC matrix element, $\mathscr{M}_{V,\nu_\alpha}^{\mathrm{NU}}$; hence we write

$$\left|\mathscr{M}_{V,\nu_\alpha}^{\mathrm{NSI}}\right|^2 = \left|\mathscr{M}_{V,\nu_\alpha}^{\mathrm{NU}}\right|^2 + \left|\mathscr{M}_{V,\nu_\alpha}^{\mathrm{FC}}\right|^2. \quad (6)$$

From experimental physics perspectives, it is rather crucial to express the differential cross section with respect to the recoil energy of the nuclear target, T_N. In recent years, it became feasible for terrestrial neutrino detectors to detect neutrino events by measuring nuclear recoil [16, 17]. Therefore, it is important to compute also the differential cross sections $d\sigma/dT_N$. In the coherent process, the nucleus recoils (intrinsically it remains unchanged) with energy which, in the approximation $T_N \ll E_\nu$, takes the maximum value $T_N^{\max} = 2E_\nu^2/(M + 2E_\nu)$, with M denoting the nuclear mass [36, 37]. Then, to a good approximation, the square of the three-momentum transfer is equal to $q^2 = 2MT_N$, and the coherent NSI differential cross section with respect to T_N can be cast in the form

$$\frac{d\sigma_{\mathrm{NSI},\nu_\alpha}}{dT_N} = \frac{G_F^2M}{\pi}\left(1 - \frac{MT_N}{2E_\nu^2}\right)\left|\langle gs|\left|G_{V,\nu_\alpha}^{\mathrm{NSI}}(q)\right||gs\rangle\right|^2. \quad (7)$$

We note that, compared to previous studies [60, 72], we have also taken into consideration the interaction ν-u quark (see (5)), in addition to the momentum dependence of the nuclear

form factors [53]. Both (4) and (7) are useful for studying the nuclear physics of NSI of neutrinos with matter.

Furthermore, by performing numerical integrations to (4) over the scattering angle θ or to (7) over the recoil energy T_N, one can obtain integrated (total) coherent NSI cross sections, $\sigma_{\mathrm{NSI},\nu_\alpha}$. Following (6), the individual cross sections $\sigma_{\mathrm{NU},\nu_\alpha}$ and $\sigma_{\mathrm{FC},\nu_\alpha}$ may be evaluated accordingly.

2.2. Standard Model Coherent ν-Nucleus Cross Sections. The effective (quark-level) SM ν-nucleus interaction Lagrangian, $\mathscr{L}_{\mathrm{SM}}$, at low and intermediate neutrino energies, is written as

$$\mathscr{L}_{\mathrm{SM}} = -2\sqrt{2}G_F \sum_{\substack{f=u,d \\ \alpha=e,\mu,\tau}} g_P^f \left[\overline{\nu}_\alpha \gamma_\rho L \nu_\alpha\right]\left[\overline{f}\gamma^\rho P f\right], \tag{8}$$

where $g_L^u = 1/2 - (2/3)\sin^2\theta_W$ and $g_R^u = -(2/3)\sin^2\theta_W$ are the left- and right-handed couplings of the u-quark to the Z-boson and $g_L^d = -1/2 + (1/3)\sin^2\theta_W$ and $g_R^d = (1/3)\sin^2\theta_W$ are the corresponding couplings of the d-quark (θ_W is the Weinberg mixing angle) [85].

For coherent ν-nucleus scattering, the SM angle-differential cross section reads

$$\frac{d\sigma_{\mathrm{SM},\nu_\alpha}}{d\cos\theta} = \frac{G_F^2}{2\pi}E_\nu^2 (1+\cos\theta)\left|\langle gs|\left|\widehat{\mathscr{M}}_0(q)\right||gs\rangle\right|^2. \tag{9}$$

The operator $\widehat{\mathscr{M}}_0$ in the nuclear matrix element of the latter equation is the Coulomb operator which is equal to the product of the zero-order spherical Bessel function times the zero-order spherical harmonic [81, 85]. This matrix element can be cast in the form [78]

$$\begin{aligned}\left|\mathscr{M}_{V,\nu_\alpha}^{\mathrm{SM}}\right|^2 &\equiv \left|\langle gs|\left|\widehat{\mathscr{M}}_0(q)\right||gs\rangle\right|^2 \\ &= \left[g_V^p Z F_Z\left(q^2\right) + g_V^n N F_N\left(q^2\right)\right]^2,\end{aligned} \tag{10}$$

where the polar-vector couplings of protons g_V^p and neutrons g_V^n with the Z-boson (see Figure 1(a)) are written as $g_V^p = 2(g_L^u + g_R^u) + (g_L^d + g_R^d) = 1/2 - 2\sin^2\theta_W$ and $g_V^n = (g_L^u + g_R^u) + 2(g_L^d + g_R^d) = -1/2$, respectively. As can be easily seen, the vector contribution of all protons is very small ($g_V^p \sim 0.04$); hence, the coherence in (10) essentially refers to all neutrons only of the studied nucleus. After some straightforward elaboration, the differential cross section with respect to the nuclear recoil energy, T_N, takes the form

$$\frac{d\sigma_{\mathrm{SM},\nu_\alpha}}{dT_N} = \frac{G_F^2 M}{\pi}\left(1 - \frac{MT_N}{2E_\nu^2}\right)\left|\langle gs|\left|\widehat{\mathscr{M}}_0(q)\right||gs\rangle\right|^2. \tag{11}$$

The Lagrangian $\mathscr{L}_{\mathrm{tot}}$ of (2) contains the flavour preserving (FP) part, equal to $\mathscr{L}_{\mathrm{FP}} \equiv \mathscr{L}_{\mathrm{NU}} + \mathscr{L}_{\mathrm{SM}}$, which can be evaluated through the Coulomb matrix element

$$\left|\mathscr{M}_{V,\nu_\alpha}^{\mathrm{FP}}\right|^2 = \left|\mathscr{M}_{V,\nu_\alpha}^{\mathrm{SM}} + \mathscr{M}_{V,\nu_\alpha}^{\mathrm{NU}}\right|^2. \tag{12}$$

Subsequently, the total coherent cross section may be computed on the basis of the matrix element

$$\left|\mathscr{M}_{V,\nu_\alpha}^{\mathrm{tot}}\right|^2 = \left|\mathscr{M}_V^{\mathrm{FP}}\right|^2 + \left|\mathscr{M}_{V,\nu_\alpha}^{\mathrm{FC}}\right|^2. \tag{13}$$

In a previous work [53], we evaluated original differential cross sections $d\sigma_{\lambda,\nu_\alpha}/d\cos\theta$ and $d\sigma_{\lambda,\nu_\alpha}/dT_N$, as well as individual angle-integrated cross sections of the form $\sigma_{\lambda,\nu_\alpha}(E_\nu)$, with $\alpha = e,\mu,\tau$ and $\lambda = \mathrm{SM}, \mathrm{NU}, \mathrm{FP}, \mathrm{FC}$ (FC stands for the six flavour changing processes $\nu_e \leftrightarrow \nu_\mu, \nu_e \leftrightarrow \nu_\tau, \nu_\mu \leftrightarrow \nu_\tau$).

In this work, we perform standard model cross sections calculations (for convenience, from now on, we drop the index $\lambda = \mathrm{SM}$ and always consider $\nu_\alpha = \nu_\beta$) for a set of nuclei throughout the periodic table up to ^{208}Pb. We adopt various nuclear models (see Section 3) to compute the nuclear form factors. Then, for a great part of the cross section results (except differential cross sections), we evaluate folded cross sections and event rates.

3. Evaluation of the Nuclear Form Factors

3.1. Nuclear Structure Calculations. At first, we study the nuclear structure details of the matrix elements entering (10); such results reflect the dependence of the coherent cross section on the incident-neutrino energy E_ν and the scattering angle θ (or the recoil energy T_N). We mention that for the even-even nuclei this study involves realistic QRPA calculations for the differential cross sections $d\sigma_{\nu_\alpha}/d\cos\theta$ and $d\sigma_{\nu_\alpha}/dT_N$, performed after constructing the nuclear ground state $|gs\rangle$ by solving iteratively the Bardeen Cooper Schrieffer (BCS) equations. The solution of these equations provides the probability amplitudes $v_{N_n}^j$ and $v_{N_n}^j$ of the jth single nucleon level to be occupied or unoccupied, respectively. Moreover, the latter equations provide the single quasiparticle energies, based on the single particle energies of the nuclear field (a Coulomb corrected Woods-Saxon potential in our case) as well as the pairing part of the residual two-body interaction (Bonn C-D potential in our case). Then, the nuclear form factors for protons (neutrons) are obtained as [78]

$$F_{N_n}\left(q^2\right) = \frac{1}{N_n}\sum_j [j]\,\langle j|j_0(qr)|j\rangle\left(v_{N_n}^j\right)^2, \tag{14}$$

with $[j] = \sqrt{2j+1}$, $N_n = Z$ (or N). For each nuclear system studied, the chosen active model space, the harmonic oscillator (h.o.) parameter b, and the values of the two parameters $g_{\mathrm{pair}}^{p(n)}$ for proton (neutron) pairs that renormalise the monopole (pairing) residual interaction (obtained from the Bonn C-D two-body potential describing the strong two-nucleon forces) are presented in Table 1. The adjustment of $g_{\mathrm{pair}}^{p(n)}$ is achieved through the reproducibility of the pairing gaps $\Delta_{p(n)}$ (see, e.g., [22]).

3.2. Other Methods for Obtaining the Nuclear Form Factors. The nuclear form factor, which is the Fourier transform of the nuclear charge density distribution $\rho_p(r)$, is defined as

$$F_Z\left(q^2\right) = \frac{4\pi}{Z}\int \rho_p(r)\, j_0(qr)\, r^2 dr, \tag{15}$$

with j_0 being the zero-order spherical Bessel function. Due to the significance of the nuclear form factors in our calculations

Table 1: The values of proton g^p_{pair} and neutron g^n_{pair} pairs that renormalise the residual interaction and reproduce the respective empirical pairing gaps Δ_p and Δ_n. The active model space and the harmonic oscillator parameter, for each isotope, are also presented.

Nucleus	Model-space	b	Δ_p	Δ_n	g^p_{pair}	g^n_{pair}
^{12}C	8 (no core)	1.522	4.68536	4.84431	1.12890	1.19648
^{16}O	8 (no core)	1.675	3.36181	3.49040	1.06981	1.13636
^{20}Ne	10 (no core)	1.727	3.81516	3.83313	1.15397	1.27600
^{28}Si	10 (no core)	1.809	3.03777	3.14277	1.15568	1.23135
^{40}Ar	15 (no core)	1.902	1.75518	1.76002	0.94388	1.01348
^{48}Ti	15 (no core)	1.952	1.91109	1.55733	1.05640	0.99890
^{76}Ge	15 (no core)	2.086	1.52130	1.56935	0.95166	1.17774
^{132}Xe	15 (core ^{40}Ca)	2.262	1.19766	1.20823	0.98207	1.13370

and for the benefit of the reader, we devote a separate discussion to summarise some useful possibilities of obtaining these observables.

3.2.1. Use of Available Experimental Data. For many nuclei and especially for odd-A isotopes, the proton nuclear form factors $F_Z(q^2)$ are computed by means of a model independent analysis (using a Fourier-Bessel expansion model or others) of the electron scattering data for the proton charge density $\rho_p(r)$ [84] wherever possible. The absence of similar data for neutron densities restricts us from assuming that $F_N(q^2) = F_Z(q^2)$. In this work, we consider this method only for the case of the very heavy doubly closed ^{208}Pb nucleus.

3.2.2. Fractional Occupation Probabilities in a Simple Shell-Model. In [87], the form factor $F_Z(q^2)$, for h.o. wavefunctions, has been written as [76, 77]

$$F_Z\left(q^2\right) = \frac{1}{Z} e^{-(qb)^2/4} \Phi\left(qb, Z\right), \qquad \Phi\left(qb, Z\right) = \sum_{\lambda=0}^{N_{\max}} \theta_\lambda \left(qb\right)^{2\lambda}. \tag{16}$$

The radial nuclear charge density distribution $\rho_p(r)$, entering the definition of (15), is written in the following compact form [76, 77]:

$$\rho_p\left(r\right) = \frac{1}{\pi^{3/2} b^3} e^{-(r/b)^2}\ \Pi\left(\frac{r}{b}, Z\right), \qquad \Pi\left(\chi, Z\right) = \sum_{\lambda=0}^{N_{\max}} f_\lambda \chi^{2\lambda}, \tag{17}$$

where $\chi = r/b$, with b denoting the h.o. size parameter. $N_{\max} = (2n + \ell)_{\max}$ stands for the number of quanta of the highest occupied proton (neutron) level. The coefficients f_λ are expressed as

$$f_\lambda = \sum_{(n,\ell)j} \frac{\pi^{1/2}\left(2j+1\right) n! C^{\lambda-\ell}_{n\ell}}{2\Gamma\left(n + \ell + 3/2\right)}, \tag{18}$$

where $\Gamma(x)$ is the Gamma function. For the coefficients θ_λ, $C^{\lambda-\ell}_{n\ell}$ and further information, see [76, 77].

Up to this point, the proton occupation probabilities entering (15) and (16) have been considered equal to unity for the states below the Fermi surface and zero for those above the Fermi surface. In [87], the authors introduced depletion and occupation numbers, to parametrise the partially occupied levels of the states. These parameters satisfy the relation

$$\sum_{\substack{(n\ell)j \\ \text{all}}} \alpha_{n\ell j}\left(2j+1\right) = N_n. \tag{19}$$

Within this context, the "active" surface nucleons (above or below the Fermi level) have nonzero occupation probability $\alpha_{n\ell j} \neq 0$, smaller than unity, while the "core" levels have occupation probability $\alpha_{n\ell j} = 1$. In this paper, we extend the work of [87] where three parameters α_1, α_2, and α_3 are used to describe the partial occupation probabilities of the surface orbits. We improve the formalism by introducing more parameters, increasing this way the number of "active" nucleons in the studied nuclear system, and come out with higher reproducibility of the experimental data [84]. To this aim, we introduce four parameters α_i, $i = 1, 2, 3, 4$, in (19). Then, the assumed "active" single-particle levels are five and (16) of [87] becomes

$$\begin{aligned}
&\Pi\left(\chi, Z, \alpha_i\right) \\
&= \Pi\left(\chi, Z_2\right)\frac{\alpha_1}{Z_1 - Z_2} + \Pi\left(\chi, Z_1\right)\left[\frac{\alpha_2}{Z_c - Z_1} - \frac{\alpha_1}{Z_1 - Z_2}\right] \\
&\quad + \Pi\left(\chi, Z_c\right)\left[\frac{Z' - Z}{Z' - Z_c} - \frac{\alpha_2}{Z_c - Z_1} - \frac{\alpha_3}{Z' - Z_c}\right] \\
&\quad + \Pi\left(\chi, Z'\right)\left[\frac{Z - Z_c}{Z' - Z_c} + \frac{\alpha_3}{Z' - Z_c} - \frac{\alpha_4}{Z'' - Z'}\right] \\
&\quad + \Pi\left(\chi, Z''\right)\left[\frac{\alpha_4}{Z'' - Z'} - \frac{\lambda}{Z''' - Z''}\right] \\
&\quad + \Pi\left(\chi, Z'''\right)\frac{\lambda}{Z''' - Z''},
\end{aligned} \tag{20}$$

with $\lambda = \alpha_1 + \alpha_2 - \alpha_3 - \alpha_4$. By substituting the polynomial $\Pi(\chi, Z)$ of (17) with that of the latter expression and using the experimental data [84], we fit the parameters α_i (and similarly for the form factor of (16)). As an example, for the ^{40}Ar isotope we have, $Z_2 = 10$, $Z_1 = 12$, $Z = Z_c = 18$,

$Z' = 20$, $Z'' = 22$, and $Z''' = 30$. The resulting fractional occupation probabilities that fit the experimental charge density distribution are $\alpha_1 = 0.85$, $\alpha_2 = 1.25$, $\alpha_3 = 0.85$, and $\alpha_4 = 0.75$. Similarly for the ^{48}Ti nucleus, we have $Z_2 = 18$, $Z_1 = 20$, $Z = Z_c = 22$, $Z' = 30$, $Z'' = 34$, and $Z''' = 40$ and the fitting parameters are $\alpha_1 = 1.0$, $\alpha_2 = 1.5$, $\alpha_3 = 0.35$, and $\alpha_4 = 0.1$. In Figure 2, the prediction of the method is compared with that of the simple shell-model and the experimental data. We note that in the momentum transfer range of our interest (i.e., $q < 2\,\mathrm{fm}^{-1}$), the form factor has excellent behaviour. We however mention that even though the FOP method presents very high reproducibility of the experimental data, it is not always applicable, for example, for deformed nuclei (where BCS appears to be still successful).

3.2.3. Use of Effective Expressions for the Nuclear Form Factors. We finally discuss one of the most accurate effective methods for calculating the nuclear form factor by [88]

$$F\left(q^2\right) = \frac{3j_1\left(qR_0\right)}{qR_0}\exp\left[-\frac{1}{2}\left(qs\right)^2\right], \tag{21}$$

where $j_1(x)$ is the known first-order spherical Bessel function and $R_0^2 = R^2 - 5s^2$, with R and s being the radius and surface thickness parameters of the nucleus, respectively. The radius parameter is usually given from the semiempirical form $R = 1.2A^{1/3}$ fm while s is of the order of 0.5 fm (see [84]).

It is worth noting that, by inserting the form factors $F_{Z(N)}$ obtained as described above in (10), the resulting cross sections have a rather high confidence level. In the next part of the paper, the results show that the momentum dependence of the nuclear form factors becomes crucial, especially for intermediate and high energies. In some cases, differences of even an order of magnitude may occur as compared to the calculations neglecting the momentum dependence of the nuclear form factors.

4. Results and Discussion

4.1. Integrated Coherent ν-Nucleus Cross Sections. The next phase of our calculational procedure is related to the total coherent ν-nucleus cross sections, obtained through numerical integration of (9) over angles (or (11) over T_N) as

$$\sigma_{\nu_\alpha}\left(E_\nu\right) = \int \frac{d\sigma_{\nu_\alpha}}{d\cos\theta}\left(\theta, E_\nu\right) d\cos\theta. \tag{22}$$

The results for the standard model cross sections, for a set of different promising targets throughout the periodic table, are presented in Figure 3. As can be seen, the present nuclear structure calculations indicate that, between light and heavy nuclear systems, the cross sections may differ by even two orders of magnitude (or more) as a consequence of the dependence on the nuclear parameters (i.e., mass, form factors, etc.). We also see that for heavier nuclei the cross sections flatten more quickly (at lower neutrino energies) compared to that of lighter nuclear isotopes. The latter conclusion originates mainly from the fact that, for heavy nuclei, the suppression of the cross sections due to the nuclear form factors becomes more significant. Thus, for heavy material, the nuclear effects become important even at low energies. Such original cross section results are helpful for the simulations of the standard and nonstandard model signals of ν-detection experiments (see below).

4.2. Supernova Neutrino Simulations. As discussed previously, our present calculations may also be useful for ongoing and future neutrino experiments related to supernova (SN) neutrino detection, since, as it is known, the neutrinos emitted in SN explosions transfer the maximum part of the total energy released. Then, the total neutrino flux, $\Phi(E_\nu)$, arriving at a terrestrial detector as a function of the SN neutrino energy E_ν, the number of emitted (anti)neutrinos N_{ν_α} at a distance d from the source (here we consider $d = 10$ kpc), reads [25, 35]

$$\Phi\left(E_\nu\right) = \sum_{\nu_\alpha}\Phi_{\nu_\alpha}\eta_{\nu_\alpha}^{\mathrm{SN}}\left(E_\nu\right) = \sum_{\nu_\alpha}\frac{N_{\nu_\alpha}}{4\pi d^2}\eta_{\nu_\alpha}^{\mathrm{SN}}\left(E_\nu\right) \tag{23}$$

($\alpha = e, \mu, \tau$) where $\eta_{\nu_\alpha}^{\mathrm{SN}}$ denotes the energy distribution of the (anti)neutrino flavour α.

The emitted SN neutrino energy spectra $\eta_{\nu_\alpha}^{\mathrm{SN}}(E_\nu)$ may be parametrised by Maxwell-Boltzmann distributions that depend only on the temperature T_{ν_α} of the (anti)neutrino flavour ν_α or $\widetilde{\nu}_\alpha$ (the chemical potential is ignored); we have

$$\eta_{\nu_\alpha}^{\mathrm{SN}}\left(E_\nu\right) = \frac{E_\nu^2}{2T_{\nu_\alpha}^3}e^{-E_\nu/T_{\nu_\alpha}} \tag{24}$$

($T_{\nu_e} = 3.5$ MeV, $T_{\widetilde{\nu}_e} = 5.0$ MeV, and $T_{\nu_x,\widetilde{\nu}_x} = 8.0$ MeV, $x = \mu, \tau$ [36]). For each flavour, the total number of emitted neutrinos N_{ν_α} is obtained from the mean neutrino energy [53]

$$\left\langle E_{\nu_\alpha}\right\rangle = 3T_{\nu_\alpha} \tag{25}$$

and the total energy released from a SN explosion, $U = 3 \times 10^{53}$ erg [18, 19].

4.3. Laboratory Neutrino Simulations. The spallation neutron source (SNS) at Oak Ridge National Lab [8] produces neutrons by firing a pulsed proton beam at a liquid mercury target [59]. The main aim of the COHERENT proposal [12, 13] (or of other similar concepts [14, 15]) concerns possible detection of neutrino-nucleus coherent scattering events at the SNS. Our simulations here are mainly motivated by previous studies [9, 16, 17, 58] and the hope to provide our accurate nuclear structure calculations.

In stopped-pion muon sources, neutrinos are produced by the pion decay chain. Pion decay at rest $\pi^+ \rightarrow \mu^+\nu_\mu$ ($\tau = 26$ ns) produces monochromatic muon neutrinos ν_μ at 29.9 MeV, followed by electron neutrinos ν_e and muon antineutrinos $\widetilde{\nu}_\mu$ that are produced by the muon decay $\mu^+ \rightarrow \nu_e e^+\widetilde{\nu}_\mu$ ($\tau = 2.2\,\mu$s) [23, 24]. For pulsed beams in time-scales narrower than μs, ν_e's and $\widetilde{\nu}_\mu$'s will be delayed with the beam while ν_μ's will be prompt with the beam [9]. The emitted ν_e

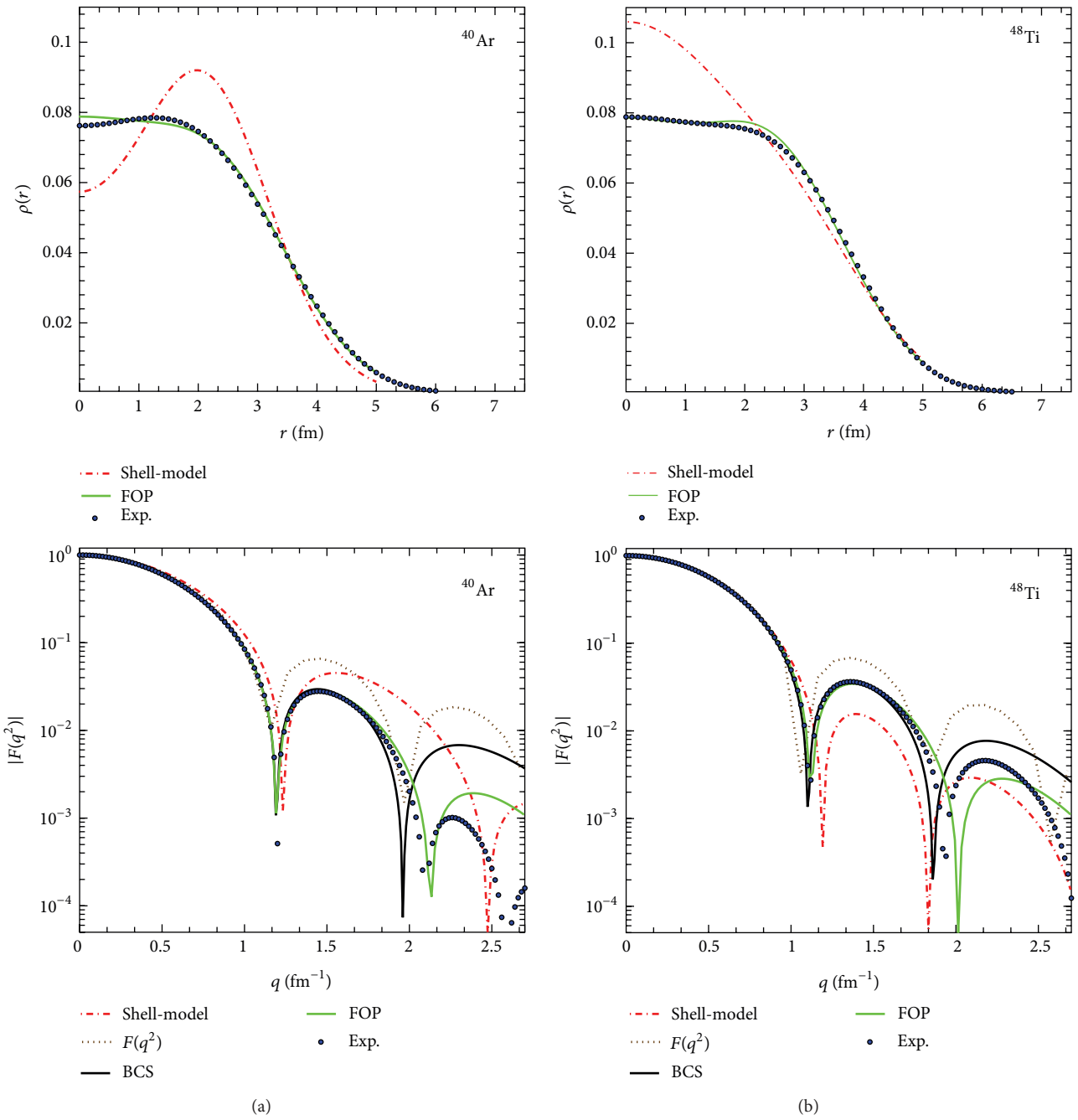

FIGURE 2: The charge density distribution (a) and the form factor as a function of the momentum transfer (b), for the cases of ^{40}Ar and ^{48}Ti nuclei. The introduction of fractional occupation probabilities (FOP) of the states provides higher reproducibility of the experimental data, compared to the simple shell-model and that of (21). The BCS nuclear neutron form factor $F_N(q^2)$ is also presented and compared.

and $\widetilde{\nu}_\mu$ neutrino spectra are described by the high precision normalized distributions, known as the Michel spectrum [11]

$$\eta_{\nu_e}^{\text{lab.}} = 96E_\nu^2 M_\mu^{-4}\left(M_\mu - 2E_\nu\right),$$
$$\eta_{\widetilde{\nu}_\mu}^{\text{lab.}} = 16E_\nu^2 M_\mu^{-4}\left(3M_\mu - 4E_\nu\right) \quad (26)$$

($M_\mu = 105.6$ MeV is the muon rest mass). The maximum neutrino energy in the latter distributions is $E_\nu^{\max} = M_\mu/2 = 52.8$ MeV (see, e.g., [10]).

The spallation neutron source (SNS) at Oak Ridge National Lab is currently the most powerful facility to detect for a first time neutrino-nucleus coherent scattering events, since it provides exceptionally intense fluxes $\Phi_{\nu_\alpha} = 2.5 \times 10^7\ \nu\text{s}^{-1}\ \text{cm}^{-2}$ at 20 m and $\Phi_{\nu_\alpha} = 6.3 \times 10^6\ \nu\text{s}^{-1}\ \text{cm}^{-2}$ at 40 m from the source [23, 24]. The simulated laboratory neutrino

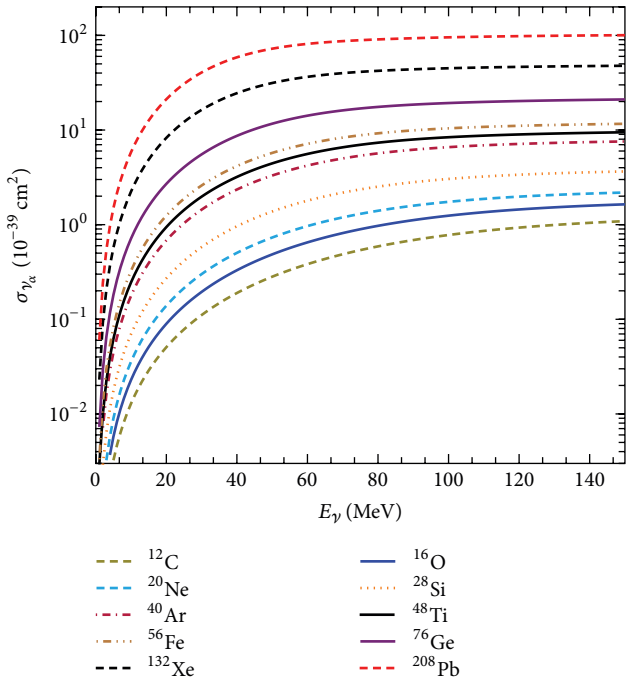

FIGURE 3: Total coherent cross sections $\sigma_{\nu_\alpha(\bar{\nu}_\alpha)}(E_\nu)$ in units 10^{-39} cm^2 for a set of nuclei as a function of the incoming neutrino energy E_ν, for the SM neutrino processes $\nu_\alpha(\bar{\nu}_\alpha) + (A, Z) \rightarrow \nu_\alpha(\bar{\nu}_\alpha) + (A, Z)$.

signals $\sigma^{\text{sign}}_{\nu,\text{lab.}}$ coming out of our calculations for the adopted nuclear targets are discussed below.

4.4. Simulated Neutrino Signals. By weighting the integrated cross section $\sigma_{\nu_\alpha}(E_\nu)$ with the neutrino distributions of (24), for SN neutrinos, or (26), for laboratory neutrinos, the total signal produced on a terrestrial detector is described by [82, 83]

$$\sigma^{\text{sign}}_{\nu,\xi}(E_\nu) = \sum_{\nu_\alpha} \sigma_{\nu_\alpha}(E_\nu)\, \eta^{\xi}_{\nu_\alpha}(E_\nu), \quad \xi = \text{SN, lab.} \tag{27}$$

The resulting signals, $\sigma^{\text{sign}}_{\nu,\xi}(E_\nu)$, obtained by inserting in (27) the cross sections σ_{ν_α} of Figure 3 are plotted in Figure 4.

In our previous work [53], it was shown that the simulated cross sections reflect the characteristics of the incident neutrino spectrum of the specific neutrino flavour α and, therefore, such a simulated signal is characterised by its own position of the maximum peak and width of the distribution $\eta^{\text{SN}}_{\nu_\alpha}$. We, however, recall that, within the framework of the SM, coherent neutrino scattering is a flavour blind and a particle-antiparticle blind process. For this particular case, our results are shown in Figure 4 for supernova and laboratory (SNS) neutrinos.

In neutrino simulations, another useful quantity is the flux averaged cross section [5] which in our notation is written as

$$\langle \sigma_\nu \rangle_\xi = \sum_{\nu_\alpha} \int \sigma_{\nu_\alpha}(E_\nu)\, \eta^{\xi}_{\nu_\alpha}(E_\nu)\, dE_\nu. \tag{28}$$

The results for $\langle \sigma_\nu \rangle_\xi$, obtained by using the angle-integrated cross sections of Figure 3, are listed in Table 2 for both neutrino sources.

4.5. Differential and Total Event Rates. From experimental physics perspectives, predictions for the differential event rate, Y_{ν_α}, of a ν-detector are crucial [25]. The usual expression for computing the yield in events is based on the neutrino flux and is defined as [35]

$$\begin{aligned} Y_{\nu_\alpha}(T_N) &= \frac{dN}{T_N} \\ &= K \sum_{\nu_\alpha} \Phi_{\nu_\alpha} \int \eta^{\xi}_{\nu_\alpha} dE_\nu \int \frac{d\sigma_{\nu_\alpha}}{d\cos\theta}\, \delta\left(T_N - \frac{q^2}{2M}\right) d\cos\theta, \end{aligned} \tag{29}$$

where $K = N_{\text{targ.}}\, t_{\text{tot.}}$ accounts for the total number of nuclei (atoms) in the detector material $N_{\text{targ.}}$ times the total time of exposure t_{tot}. Using the latter equation, one concludes that the lower the energy recoil, the larger the potentially detected number of events (see Figures 5 and 6). In principle, in order to maximize the potential detection of a rare event process like the ν-nucleus scattering, detector materials with very-low-energy recoil threshold and low-background are required.

In the last stage of our study, we make predictions for the total number of coherent scattering events, the most important quantity, both from theoretical and from experimental perspectives. To this purpose, we evaluate the number

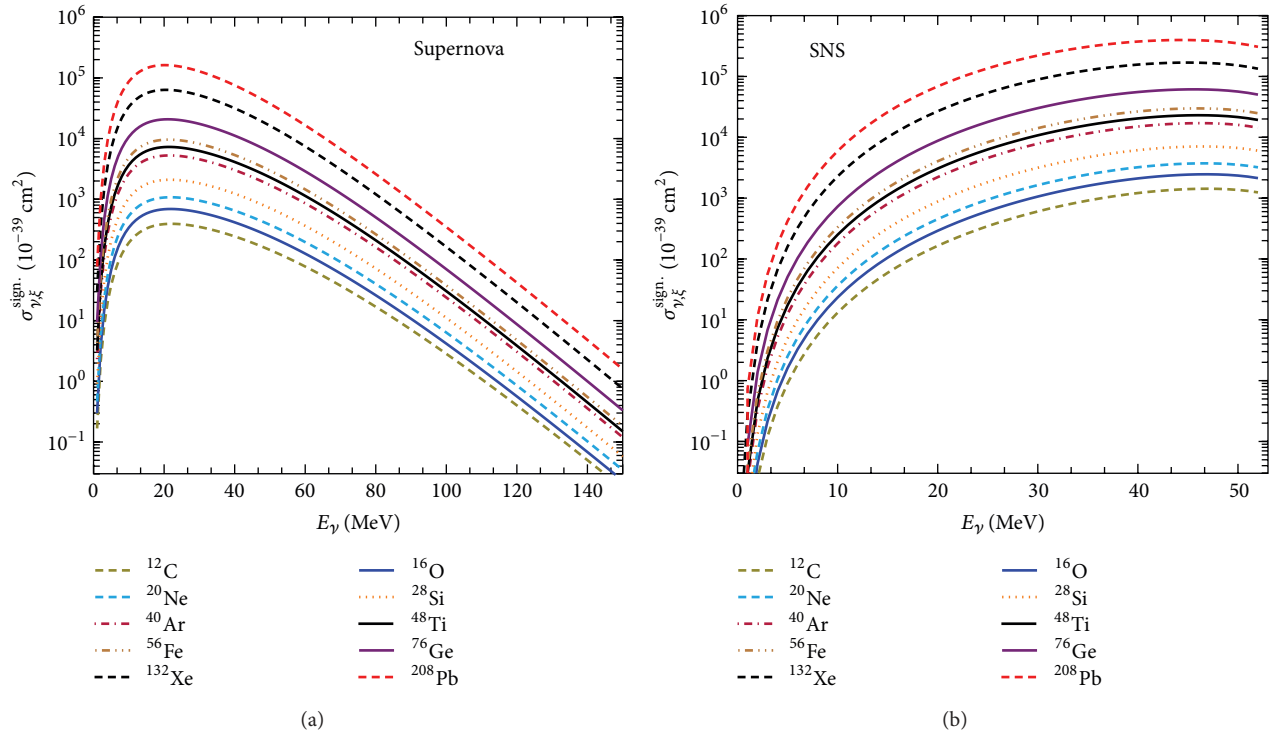

Figure 4: The signal cross sections that represent the expected signal to be recorded on a terrestrial nuclear ν-detector, (a) for supernova neutrinos (ξ = SN), evaluated with Maxwell-Boltzmann distributions at d = 10 kpc, and (b) for SNS neutrinos (ξ = lab.), at 20 m from the source. For the case of SNS neutrinos, the figure takes into account only the delayed beam, evaluated with the generic flux of $\Phi_{\nu_\alpha} \sim 10^7\ \nu\text{s}^{-1}\ \text{cm}^{-2}$. Different nuclear detectors have been studied.

Table 2: Flux averaged cross sections $\langle\sigma_\nu\rangle_\xi$ in units 10^{-40} cm^2 for the adopted supernova (d = 10 kpc) and laboratory (delayed flux only) neutrino spectra. For the case of SNS neutrinos, we adopt the generic flux, that is, $\Phi_{\nu_\alpha} \sim 10^7\ \nu\text{s}^{-1}\ \text{cm}^{-2}$ at 20 m for all nuclear targets.

Nucleus	^{12}C	^{16}O	^{20}Ne	^{28}Si	^{40}Ar	^{48}Ti	^{56}Fe	^{76}Ge	^{132}Xe	^{208}Pb
$\langle\sigma_\nu\rangle_{\text{SN}}$	1.46	2.51	3.91	7.52	18.59	25.43	33.29	70.63	207.56	514.93
$\langle\sigma_\nu\rangle_{\text{lab.}}$	3.07	5.33	8.13	15.52	37.91	51.50	67.02	139.83	395.59	949.50

Table 3: Total number of events per ton of the target materials for a supernova at a distance of 10 kpc. We assume various energy thresholds 5, 10, 25, or 50 keV. Our present results are in excellent agreement with those of [25, 35].

Nucleus	T_N	$T_N > 5$ keV	$T_N > 10$ keV	$T_N > 25$ keV	$T_N > 50$ keV
^{12}C	2.52	2.25	2.05	1.60	1.14
^{16}O	3.29	2.84	2.51	1.83	1.19
^{20}Ne	4.03	3.35	2.87	1.96	1.16
^{40}Ar	9.46	6.63	5.01	2.53	1.00
^{48}Ti	10.73	7.04	5.06	2.27	0.76
^{56}Fe	12.00	7.36	5.04	2.01	0.57
^{76}Ge	18.58	9.61	5.82	1.70	0.30
^{132}Xe	30.68	9.84	4.16	0.46	0.01
^{208}Pb	46.93	7.86	1.95	0.03	$<10^{-3}$

of expected counts, for the studied detector materials, by performing numerical integration of (29) over the nuclear recoil threshold $T_N^{\text{thres.}}$ (see Table 3).

As has been discussed previously [25, 26], SN neutrino detection might become possible by the massive dark matter detectors [32] which have very good energy resolution and low threshold capabilities [35]. These experiments are designed (or planned) to search for WIMPs [27–29] and/or other rare events such as the neutrinoless double beta decay. The latter use heavy nuclei as nuclear detectors, for example, Ge (GERDA [31] and SuperCDMS [30] experiments). In addition, we report that SN neutrino events can be potentially

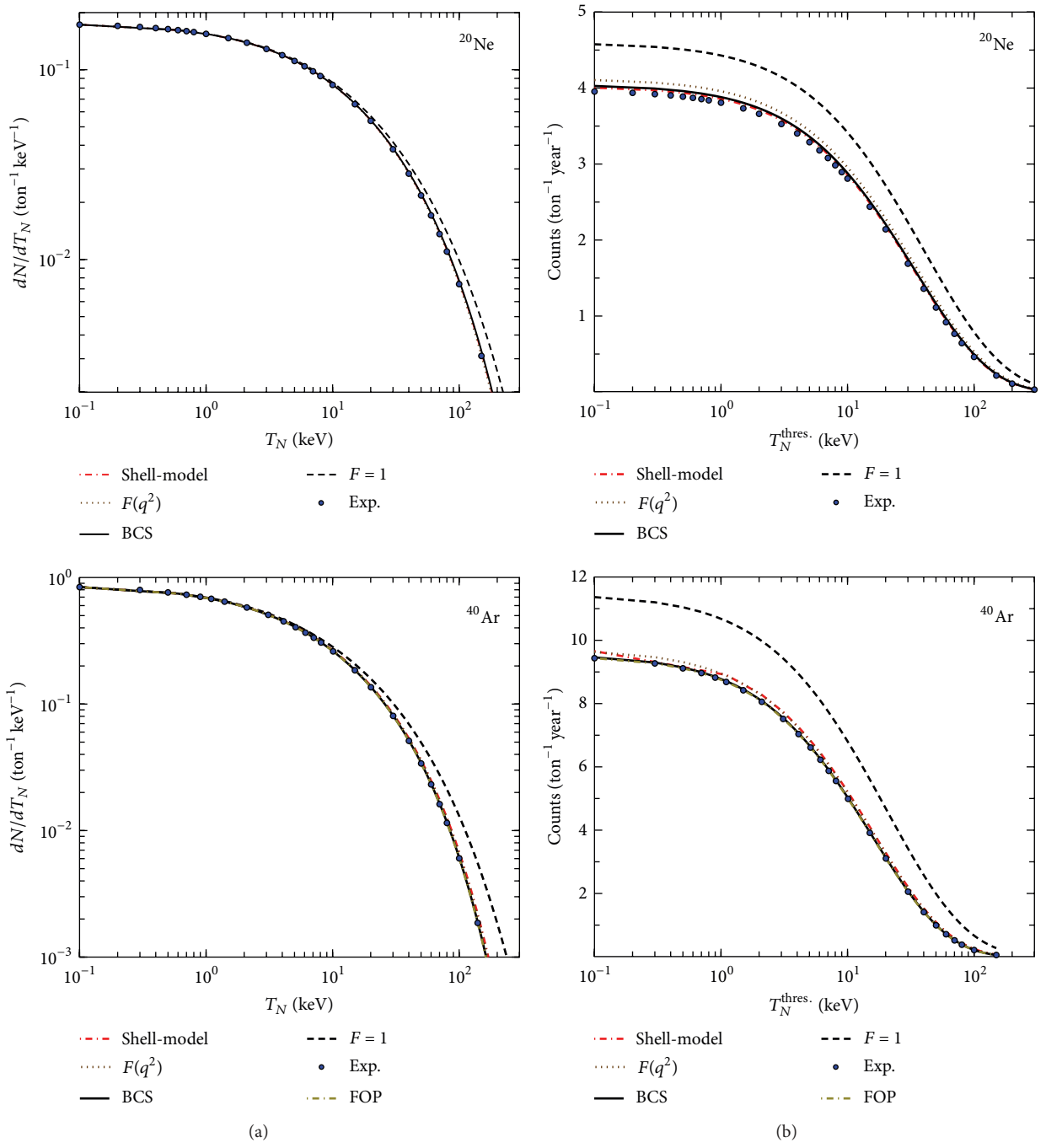

FIGURE 5: Yield in events (a) and total number of events over nuclear recoil threshold $T_N^{\text{thres.}}$ (b), for supernova neutrinos at $d = 10$ kpc. Here, 1 ton of perfectly efficient ^{20}Ne and ^{40}Ar detectors has been considered and also possible effects of neutrino oscillation in propagation are neglected. For heavier nuclear targets the differences become rather significant. In this figure, $F(q^2)$ stands for (21) and FOP for the method of fractional occupation probabilities of the states. For more details, see the text.

detected by experiments using noble gases like Ne (CLEAN detector [32]), Ar (WARP programme [33]), and Xe (XENON 100 Collaboration [34]).

As mentioned in Section 3, in order to test our nuclear calculations, we have also employed other nuclear methods. To this purpose, we have compared our original results evaluated with the BCS method with those obtained as discussed in Section 3.2 and concluded that for the case of the coherent channel all available nuclear methods are in good agreement, but their results differ significantly from those obtained assuming $F_Z(q^2) = F_N(q^2) = 1$ (see Figures 5 and 6). We stress, however, the fact that since the cross section is mostly sensitive to the neutron distribution of the target nucleus, the most accurate method (at low and

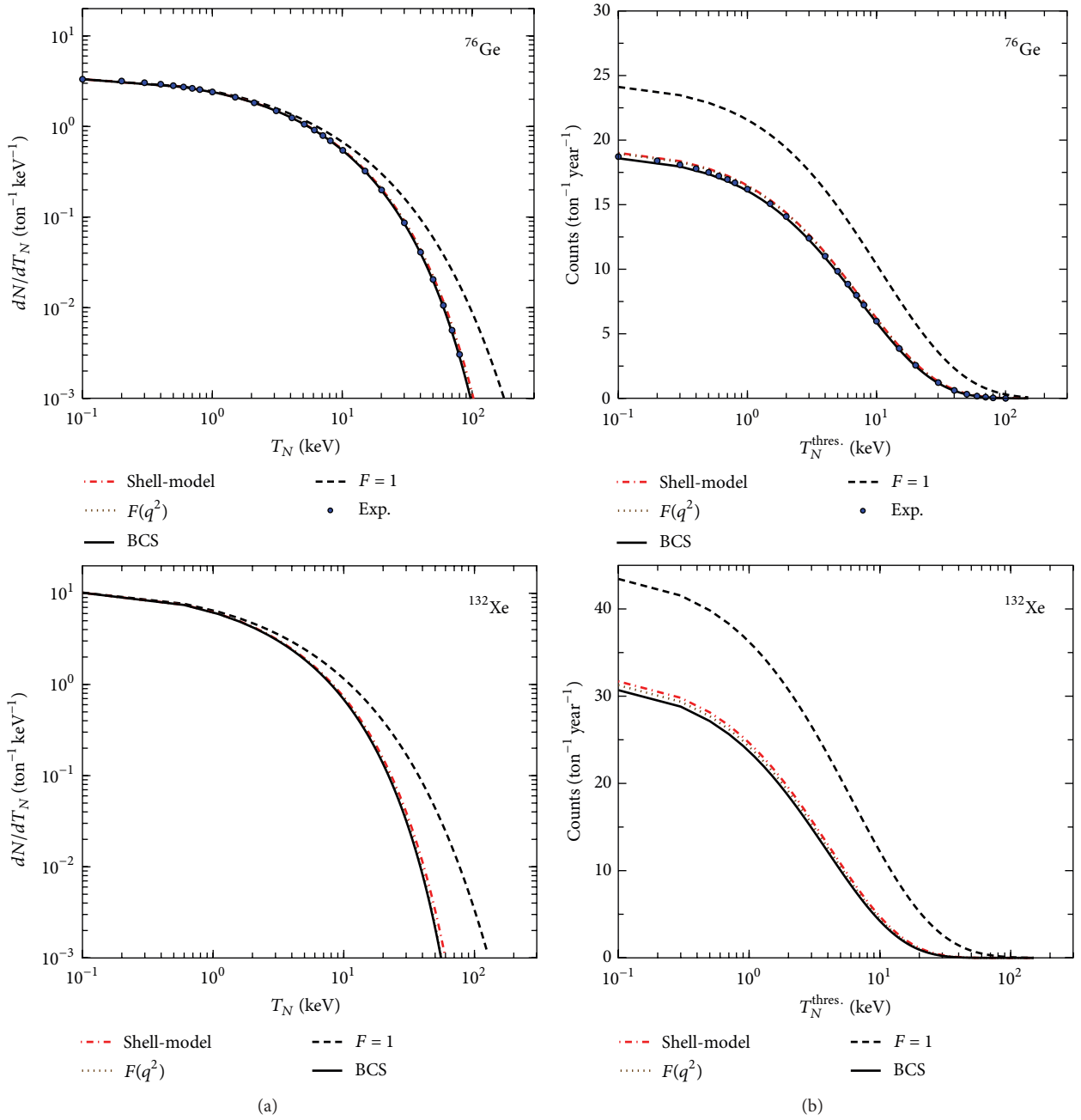

FIGURE 6: Same as Figure 5 but for ^{76}Ge and ^{132}Xe.

intermediate energies) is the BCS method which provides realistic proton as well as neutron form factors. All other methods employed here consider only the proton distribution and assume $F_Z(q^2) = F_N(q^2)$, which, especially for heavy nuclei, is a rather crude approximation. We remark, however, that the aforementioned nuclear methods offer reliable results on the differential and total event rates for low energies (see Figures 5 and 6), but in order to correctly estimate the neutron form factor, methods like the BSC are probably more appropriate.

Our present nuclear structure calculations for laboratory (SNS) neutrinos [8] (see Figure 7) are in good agreement with previous results [9]. They imply that a comparably large number of coherent neutrino scattering events are expected to be measured by using LNe, LAr, LXe, Ge, and CsI[Na] materials adopted by the COHERENT Collaboration [12, 13]. The predictions of the BCS method for these nuclei are illustrated in Figure 7 and compared with those of other promising nuclear targets. Because the neutrino flux produced at the SNS is very high (of the order of $\Phi_{\nu_\alpha} \sim 10^7\ \nu s^{-1}\ cm^{-2}$ per flavour at 20 m from the source [23]), even kg-scale experiments expect to measure neutrino-nucleus coherent scattering events at significantly higher rates than those of supernova neutrinos.

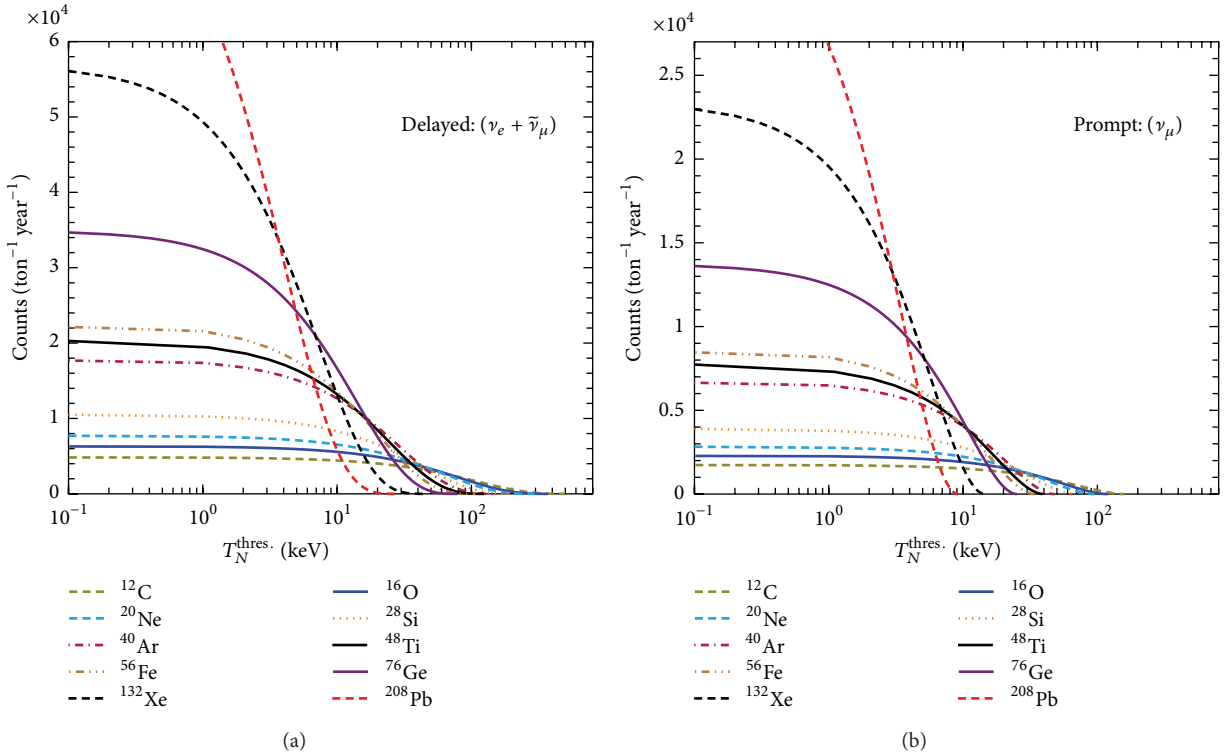

FIGURE 7: Total number of expected events over nuclear recoil threshold for 1 ton of various nuclear targets at 20 m from the source ($\Phi_{\nu_\alpha} \sim 10^7\ \nu s^{-1}\ cm^{-2}$). The left (right) panel assumes the delayed (prompt) flux of laboratory stopped-pion neutrino sources. This figure assumes a perfectly efficient detector and negligible neutrino oscillation effects.

It is worth noting that the choice of the target nucleus plays also a crucial role, since a light nuclear target may yield almost constant number of events throughout the energy range, but small number of counts. On the other hand, a heavy nuclear target provides more counts but yields low-energy recoil, making the detection more difficult. This leads to the conclusion that the most appropriate choice for a nuclear detector might be a combination of light and heavy nuclear isotopes, like the scintillation detectors discussed in [35].

4.6. Nonstandard Neutrino Interactions at the COHERENT Detector. The multitarget approach of the COHERENT experiment [12, 13] aiming at neutrino detection can also explore nonstandard physics issues such as NSI [52, 53], neutrino magnetic moment [57], and sterile neutrino [58]. In this subsection, we find it interesting to evaluate the nonstandard neutrino-nucleus events that could be potentially detected by this experiment in each of the proposed nuclear targets. The high intensity SNS neutrino beams [8] and the two promising ν-detectors, liquid ^{20}Ne (391 kg) and liquid ^{40}Ar (456 kg) [58], firstly proposed by the CLEAR [14] and CLEAN [32] designs (located at distance 20 m from the source), constitute excellent probes to search for the exotic ν-reactions. Other possibilities [12, 13] include medium and heavy weight targets like ^{76}Ge (100 kg) inspired by the dark matter SuperCDMS [30] detector (located at 20 m) and ^{132}Xe (100 kg located at 40 m).

In Figures 8 and 9, the resulting number of exotic events is illustrated and compared with the SM predictions. We note, however, that, especially for the case of the flavour changing (FC) channel $\nu_\mu \to \nu_e$, by using the extremely high sensitivity of the ongoing $\mu^- \to e^-$ conversion experiments (COMET [43, 44] and Mu2e [47]), very robust bounds have been set on the vector parameters $\epsilon_{\mu e}^{fV}$ [53]. To this end, we conclude that if the Mu2e and COMET experiments will not detect muon-to-electron conversion events, then the new $\epsilon_{\mu e}^{fV}$ parameters extracted in [53] will lead to undetectable coherent rates at the SNS facility for this channel.

For our present calculations we used the current bounds [53] set by the sensitivity of the PSI experiment [89] and found countable number of events for the near detectors in the case of the corresponding $\nu_\mu \to \nu_e$ reaction. The other exotic parameters, that is, $\epsilon_{\alpha\alpha}^{fV}$ with $\alpha = e, \mu$ and $\epsilon_{e\tau}^{fV}$, have been taken from [51]. As discussed in [53], we do not take into account the $\epsilon_{\tau\tau}^{fV}$ contribution, since the corresponding limits are poorly constrained and eventually predict unacceptably high rates.

Before closing, it is worth noting that the present calculations indicate significant possibility of detecting exotic neutrino-nucleus events through coherent scattering in the aforementioned experiments. Since neutrino-physics enters a precision era [9], a difference from the standard model

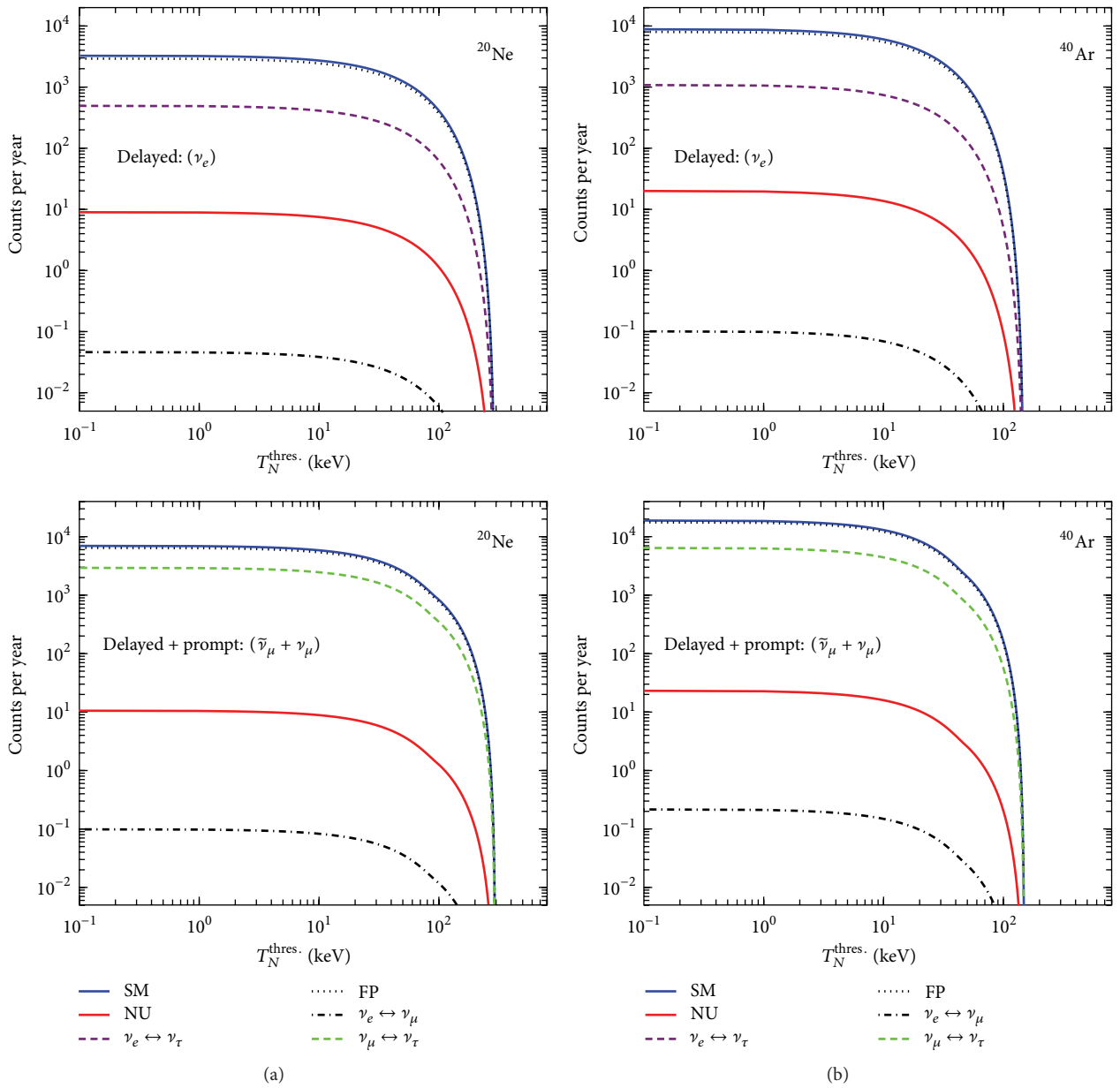

FIGURE 8: The expected nonstandard neutrino scattering events over the recoil energy threshold at the COHERENT detector, filled with (a) 391 kg of liquid ^{20}Ne and (b) 456 kg of liquid ^{40}Ar, both located at a distance of 20 m ($\Phi_{\nu_\alpha} = 2.5 \times 10^7\ \nu s^{-1}\ cm^{-2}$) from the source. A perfectly efficient detector and negligible neutrino oscillation effects are assumed.

predictions leads to undoubtable evidence of nonstandard neutrino-nucleus interactions (NSI). We recall that, in order to experimentally constrain simultaneously all the exotic parameters at high precision, the detector material should consist of maximally different ratio $k = (A + N)/(A + Z)$ [9, 52].

Our future plans include estimation of the incoherent channel which may provide a significant part of the total cross section, especially for energies higher than $E_\nu \approx 20$–40 MeV (depending on the nuclear target [81] and the particle model predicting the exotic process).

5. Summary and Conclusions

Initially, in this paper, the evaluation of all required nuclear matrix elements, related to standard model and exotic neutral-current ν-nucleus processes, is formulated, and realistic nuclear structure calculations of ν-nucleus cross sections for a set of interesting nuclear targets are performed. The first stage involves cross sections calculations for the dominant coherent channel in the range of incoming neutrino-energies $0 \leq E_\nu \leq 150$ MeV (it includes ν-energies of stopped-pion muon neutrino decay sources, supernova neutrinos, etc.).

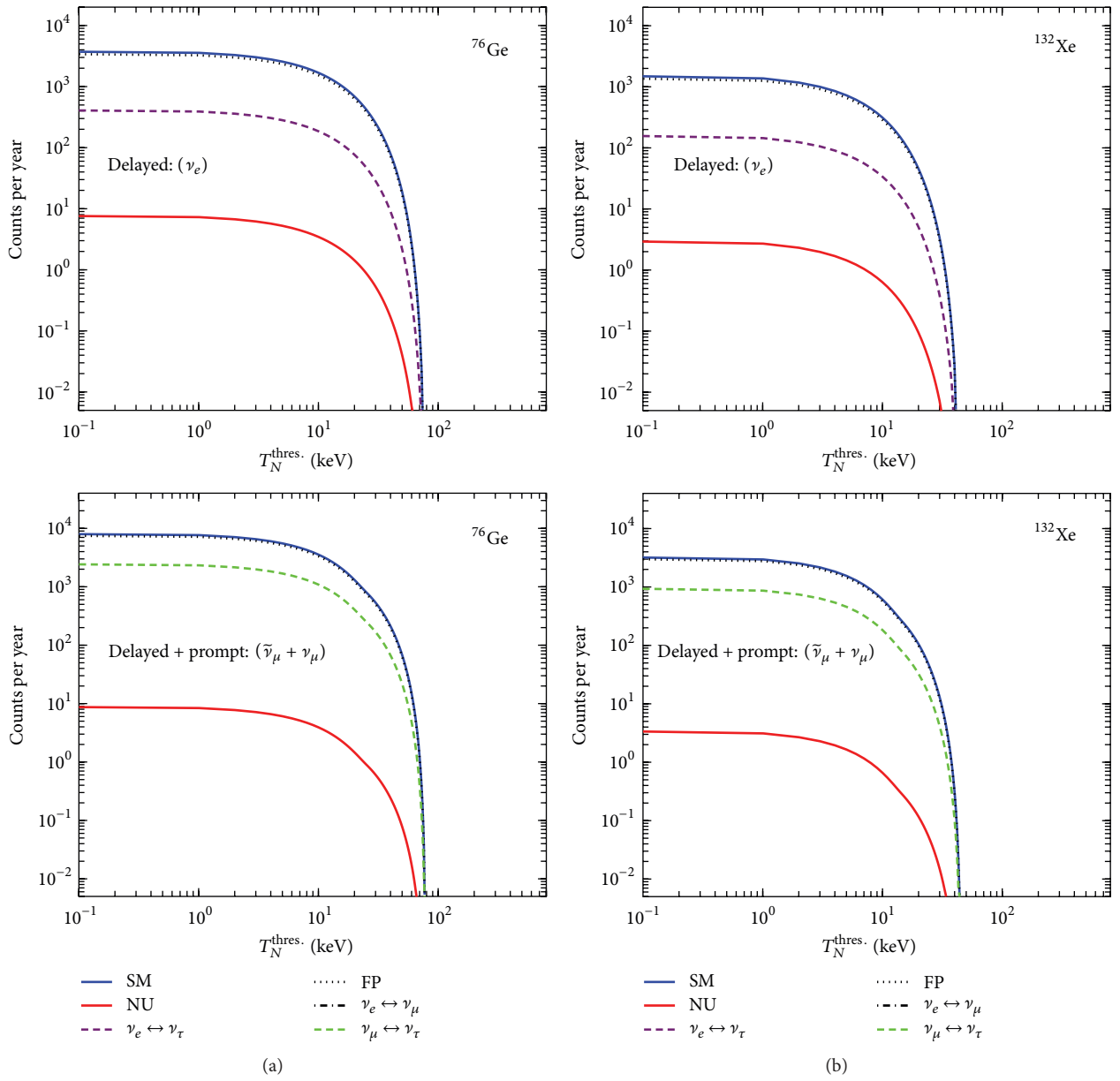

FIGURE 9: Same as Figure 8, but for 100 kg of ^{76}Ge at 20 m ($\Phi_{\nu_\alpha} = 2.5 \times 10^7\ \nu s^{-1}\ cm^{-2}$) and 100 kg of liquid ^{132}Xe at 40 m ($\Phi_{\nu_\alpha} = 6.3 \times 10^6\ \nu s^{-1}\ cm^{-2}$) from the source.

Additionally, new results for the total number of events expected to be observed in one ton of various ν-detector materials are provided and the potentiality of detecting supernova as well as laboratory neutrino-nucleus events is in detail explored. The calculations are concentrated on interesting nuclei, like ^{20}Ne, ^{40}Ar, ^{76}Ge, and ^{132}Xe, which are important detector materials for several rare event experiments, like the COHERENT at Oak Ridge National Laboratory, and also experiments searching for dark matter events as the GERDA, SuperCDMS, XENON 100, CLEAN, and so forth. By comparing our results with those of other methods, we see that the nuclear physics aspects (reflecting the accuracy of the required ν-nucleus cross sections) appreciably affect the coherent $gs \rightarrow gs$ transition rate, a result especially useful for supernova ν-detection probes.

In the present work, the QRPA method that considers realistic nuclear forces has been adopted in evaluating the nuclear form factors, for both categories of ν-nucleus processes, the conventional and the exotic ones. Also, a comparison with other simpler methods as (i) effective methods and (ii) the method of fractional occupation probabilities, which improves over the simple shell-model and gives higher reproducibility of the available experimental data, is presented and discussed. We conclude that among all the adopted methods the agreement is quite good, especially for light and medium nuclear isotopes. However, since coherent

neutrino-nucleus scattering can probe the neutron nuclear form factors, methods like the BCS provide more reliable results.

In view of the operation of extremely intensive neutrino fluxes (at the SNS, PSI, J-PARC, Fermilab, etc.), the sensitivity to search for new physics will be largely increased, and therefore, through coherent neutrino-nucleus scattering cross section measurements, several open questions (involving nonstandard neutrino interactions, neutrino magnetic moment, sterile neutrino searches, and others) may be answered. Towards this purpose, we have comprehensively studied the nonstandard neutrino-nucleus processes and provided results for interesting nuclear detectors. Our predictions for the total number of events indicate that, within the current limits of the respective flavour violating parameters, the COHERENT experiment may come out with promising results on NSI. Moreover, this experiment in conjunction with the designed sensitive muon-to-electron conversion experiments (Mu2e, COMET) may offer significant contribution for understanding the fundamental nature of electroweak interactions in the leptonic sector and for constraining the parameters of beyond the SM Lagrangians.

Conflict of Interests

The authors declare that there is no conflict of interests regarding the publication of this paper.

Acknowledgment

One of the authors, D. K. Papoulias, wishes to thank Dr. O. T. Kosmas for technical assistance.

References

[1] D. Z. Freedman, "Coherent effects of a weak neutral current," *Physical Review D*, vol. 9, no. 5, pp. 1389–1392, 1974.

[2] A. Drukier and L. Stodolsky, "Principles and applications of a neutral-current detector for neutrino physics and astronomy," *Physical Review D*, vol. 30, no. 11, pp. 2295–2309, 1984.

[3] K. Langanke, "Weak interaction, nuclear physics and supernovae," *Acta Physica Polonica B*, vol. 39, no. 2, p. 265, 2008.

[4] H. Ejiri, "Nuclear spin isospin responses for low-energy neutrinos," *Physics Reports*, vol. 338, no. 3, pp. 265–351, 2000.

[5] T. S. Kosmas and E. Oset, "Charged current neutrino-nucleus reaction cross sections at intermediate energies," *Physical Review C: Nuclear Physics*, vol. 53, no. 3, pp. 1409–1415, 1996.

[6] J. Schechter and J. W. F. Valle, "Neutrino Masses in SU(2) x U(1) Theories," *Physical Review D*, vol. 22, no. 9, pp. 2227–2235, 1980.

[7] J. Schechter and J. W. F. Valle, "Neutrino decay and spontaneous violation of lepton number," *Physical Review D*, vol. 25, p. 774, 1982.

[8] http://www.phy.ornl.gov/nusns.

[9] K. Scholberg, "Prospects for measuring coherent neutrino-nucleus elastic scattering at a stopped-pion neutrino source," *Physical Review D*, vol. 73, Article ID 033005, 2006.

[10] A. A. Aguilar-Arevalo, C. E. Anderson, A. O. Bazarko et al., "Neutrino flux prediction at MiniBooNE," *Physical Review D*, vol. 79, no. 7, Article ID 072002, 38 pages, 2009.

[11] W. C. Louis, "Searches for muon-to-electron (anti) neutrino flavor change," *Progress in Particle and Nuclear Physics*, vol. 63, no. 1, pp. 51–73, 2009.

[12] A. Bolozdynya, F. Cavanna, Y. Efremenko et al., "Opportunities for neutrino physics at the spallation neutron source: a white paper," http://arxiv.org/abs/1211.5199.

[13] D. Akimov, A. Bernstein, P. Barbeau et al., "Coherent scattering investigations at the spallation neutron source: a snowmass white paper," http://arxiv.org/abs/1310.0125.

[14] K. Scholberg, T. Wongjirad, E. Hungerford et al., "The CLEAR experiment," http://arxiv.org/abs/0910.1989.

[15] J. Yoo, Measuring coherent-NCν as at Fermilab, 2011, http://if-neutrino.fnal.gov/neutrino1-pagers.pdf.

[16] S. J. Brice, "A method for measuring coherent elastic neutrino-nucleus scattering at a far off-axis high-energy neutrino beam target," *Physical Review D*, vol. 89, no. 7, Article ID 072004, 20 pages, 2014.

[17] J. I. Collar, N. E. Fields, E. Fuller et al., "Coherent neutrino-nucleus scattering detection with a CsI[Na] scintillator at the SNS spallation source," http://arxiv.org/abs/1407.7524.

[18] K. Hirata, T. Kajita, M. Koshiba et al., "Observation of a neutrino burst from the supernova SN1987A," *Physical Review Letters*, vol. 58, p. 1490, 1987.

[19] R. M. Bionta, G. Blewitt, C. B. Bratton et al., "Observation of a neutrino burst in coincidence with supernova 1987a in the large magellanic cloud," *Physical Review Letters*, vol. 58, no. 14, pp. 1494–1496, 1987.

[20] M. T. Keil, G. G. Raffelt, and H.-T. Janka, "Monte Carlo study of supernova neutrino spectra formation," *Astrophysical Journal Letters*, vol. 590, no. 2 I, pp. 971–991, 2003.

[21] W. C. Haxton, "Radiochemical neutrino detection via $^{127}|\,(\nu_e, e^-)^{127} \times e$," *Physical Review Letters*, vol. 60, no. 9, pp. 768–771, 1988.

[22] P. G. Giannaka and T. S. Kosmas, "Electron-capture and its role to explosive neutrino-nucleosynthesis," *Journal of Physics: Conference Series*, vol. 410, Article ID 012124, 2013.

[23] F. T. Avignone III and Y. V. Efremenko, "Neutrino-nucleus cross-section measurements at intense, pulsed spallation sources," *Journal of Physics G: Nuclear and Particle Physics*, vol. 29, no. 11, pp. 2615–2628, 2003.

[24] Y. Efremenko and W. Hix, "Opportunities for neutrino physics at the Spallation Neutron Source (SNS)," *Journal of Physics: Conference Series*, vol. 173, no. 1, Article ID 012006, 2009.

[25] C. J. Horowitz, K. J. Coakley, and D. N. McKinsey, "Supernova observation via neutrino-nucleus elastic scattering in the CLEAN detector," *Physical Review D*, vol. 68, no. 2, Article ID 023005, 7 pages, 2003.

[26] A. J. Anderson, J. M. Conrad, E. Figueroa-Feliciano, K. Scholberg, and J. Spitz, "Coherent neutrino scattering in dark matter detectors," *Physical Review D: Particles, Fields, Gravitation and Cosmology*, vol. 84, no. 1, Article ID 013008, 2011.

[27] T. S. Kosmas and J. D. Vergados, "Cold dark matter in SUSY theories: the role of nuclear form factors and the folding with the LSP velocity," *Physical Review D: Particles, Fields, Gravitation and Cosmology*, vol. 55, no. 4, pp. 1752–1764, 1997.

[28] J. D. Vergados and T. S. Kosmas, "Muon-number-violating processes in nuclei," *Physics of Atomic Nuclei*, vol. 61, p. 1066, 1998.

[29] J. D. Vergados and T. S. Kosmas, "Searches for cold dark-matter—a case of the coexistence of supersymmetry and nuclear-physics," *Physics of Atomic Nuclei*, vol. 61, no. 7, pp. 1066–1080, 1998.

[30] P. Brink, B. Cabrera, and C. L. Chang, "Beyond the CDMS-II dark matter search: superCDMS," in *Proceedings of the 22nd Texas Symposium on Rela Conference*, Stanford, Calif, USA, December 2004.

[31] GERDA Collaboration, "The GERDA experiment at Gran Sasso," *Acta Physica Polonica B*, vol. 41, pp. 1469–1476, 2010.

[32] D. N. McKinsey and K. J. Coakley, "Neutrino detection with CLEAN," *Astroparticle Physics*, vol. 22, no. 5-6, pp. 355–368, 2005.

[33] R. Brunetti, E. Calligarich, M. Cambiaghi et al., "WARP liquid argon detector for dark matter survey," *New Astronomy Reviews*, vol. 49, no. 2–6, pp. 265–269, 2005.

[34] XENON100 Collaboration, "The XENON100 dark matter experiment," http://arxiv.org/abs/1107.2155v1.

[35] M. Biassoni and C. Martinez, "Study of supernova ν-nucleus coherent scattering interactions," *Astroparticle Physics*, vol. 36, pp. 151–155, 2012.

[36] Y. Giomataris and J. D. Vergados, "A network of neutral current spherical TPCs for dedicated supernova detection," *Physics Letters B: Nuclear, Elementary Particle and High-Energy Physics*, vol. 634, no. 1, pp. 23–29, 2006.

[37] J. Monroe and P. Fisher, "Neutrino backgrounds to dark matter searches," *Physical Review D*, vol. 76, Article ID 033007, 2007.

[38] S. Fukuda, Y. Fukuda, M. Ishitsuka et al., "Solar ^8B and hep Neutrino Measurements from 1258 Days of Super-Kamiokande Data," *Physical Review Letters*, vol. 86, no. 25, pp. 5651–5655, 2001.

[39] Q. R. Ahmad, R. C. Allen, T. C. Andersen et al., "Measurement of day and night neutrino energy spectra at SNO and constraints on neutrino mixing parameters," *Physical Review Letters*, vol. 89, Article ID 011302, 2002.

[40] K. Eguchi, S. Enomoto, K. Furuno et al., "First results from KamLAND: evidence for reactor antineutrino disappearance," *Physical Review Letters*, vol. 90, no. 2, 6 pages, 2003.

[41] D. V. Forero, M. Tortola, and J. W. F. Valle, "Global status of neutrino oscillation parameters after Neutrino-2012," *Physical Review D*, vol. 86, Article ID 073012, 2012.

[42] J. W. F. Valle, "Understanding and probing neutrinos," *Nuclear Physics B—Proceedings Supplements*, vol. 229–232, pp. 23–29, 2012.

[43] Y. G. Cui, R. Palmer, Y. Arimoto et al., "KEK Report 2009-10".

[44] COMET Collaboration, The COMET Proposal to JPARC, JPARC Proposal, 2007.

[45] R. J. Abrams, D. Alezander, G. Ambrosio et al., "Mu2e conceptual design report," http://arxiv.org/abs/1211.7019.

[46] Mu2e Collaboration and F. Cervelli, "The Mu2e experiment at Fermilab," *Journal of Physics: Conference Series*, vol. 335, no. 1, Article ID 012073, 2011.

[47] R. H. Bernstein and P. S. Cooper, "Charged lepton flavor violation: an experimenter's guide," *Physics Reports*, vol. 532, no. 2, pp. 27–64, 2013.

[48] R. J. Barlow, "The PRISM/PRIME project," *Nuclear Physics B—Proceedings Supplements*, vol. 218, no. 1, pp. 44–49, 2011.

[49] Y. Kuno, "COMET and PRISM—search for charged Lepton flavor violation with muons," *Nuclear Physics B—Proceedings Supplements*, vol. 225-227, pp. 228–231, 2012.

[50] Y. Kuno and Y. Okada, "Muon decay and physics beyond the standard model," *Reviews of Modern Physics*, vol. 73, p. 151, 2001.

[51] S. Davidson, C. Pena-Garay, N. Rius, and A. Santamaria, "Present and future bounds on non-standard neutrino interactions," *Journal of High Energy Physics*, vol. 2003, no. 03, article 011, 2003.

[52] J. Barranco, O. G. Miranda, and T. I. Rashba, "Probing new physics with coherent neutrino scattering off nuclei," *Journal of High Energy Physics*, vol. 2005, article 021, 2005.

[53] D. K. Papoulias and T. S. Kosmas, "Nuclear aspects of neutral current non-standard ν-nucleus reactions and the role of the exotic $\mu^- \to e^-$ transitions experimental limits," *Physics Letters B*, vol. 728, pp. 482–488, 2014.

[54] A. Friedland, C. Lunardini, and C. Peña-Garay, "Solar neutrinos as probes of neutrino–matter interactions," *Physics Letters B*, vol. 594, no. 3-4, pp. 347–354, 2004.

[55] A. Friedland, C. Lunardini, and M. Maltoni, "Atmospheric neutrinos as probes of neutrino-matter interactions," *Physical Review D: Particles, Fields, Gravitation and Cosmology*, vol. 70, no. 11, Article ID 111301, pp. 1–111301, 2004.

[56] A. Friedland, C. Lunardini, and D. Phys. Rev, "Test of tau neutrino interactions with atmospheric neutrinos and K2K data," *Physical Review D*, vol. 72, no. 5, Article ID 053009, 16 pages, 2005.

[57] K. J. Healey, A. A. Petrov, and D. Zhuridov, "Nonstandard neutrino interactions and transition magnetic moments," *Physical Review D*, vol. 87, Article ID 117301, 11 pages, 2013.

[58] A. J. Anderson, J. M. Conrad, E. Figueroa-Feliciano et al., "Measuring active-to-sterile neutrino oscillations with neutral current coherent neutrino-nucleus scattering," *Physical Review D: Particles, Fields, Gravitation and Cosmology*, vol. 86, no. 1, Article ID 013004, 2012.

[59] P. S. Amanik and G. C. McLaughlin, "Nuclear neutron form factor from neutrino-nucleus coherent elastic scattering," *Journal of Physics G: Nuclear and Particle Physics*, vol. 36, no. 1, Article ID 015105, 2009.

[60] P. S. Amanik, G. M. Fuller, and B. Grinstein, "Flavor changing supersymmetry interactions in a supernova," *Astroparticle Physics*, vol. 24, no. 1-2, pp. 160–182, 2005.

[61] A. Esteban-Pretel, R. Tomas, and J. W. F. Valle, "Interplay between collective effects and nonstandard interactions of supernova neutrinos," *Physical Review D*, vol. 81, no. 6, Article ID 063003, 16 pages, 2010.

[62] D. K. Papoulias and T. S. Kosmas, "Exotic lepton flavour violating processes in the presence of nuclei," *Journal of Physics: Conference Series*, vol. 410, Article ID 012123, 2013.

[63] H. C. Chiang, E. Oset, T. S. Kosmas, A. Faessler, and J. D. Vergados, "Coherent and incoherent (μ^-, e$^-$) conversion in nuclei," *Nuclear Physics A*, vol. 559, no. 4, pp. 526–542, 1993.

[64] T. S. Kosmas and J. D. Vergados, "(μ^-, e$^-$) conversion: a symbiosis of particle and nuclear physics," *Physics Report*, vol. 264, no. 1–5, pp. 251–266, 1996.

[65] T. S. Kosmas, "Exotic $\mu^- \to$ e$^-$ conversion in nuclei: energy moments of the transition strength and average energy of the outgoing e$^-$," *Nuclear Physics A*, vol. 683, no. 1–4, pp. 443–462, 2001.

[66] T. S. Kosmas, "Current nuclear physics issues in studying the neutrinoless (μ^-, e$^-$) conversion in nuclei," *Progress in Particle and Nuclear Physics*, vol. 48, pp. 307–316, 2002.

[67] T. S. Kosmas, G. K. Leontaris, and J. D. Vergados, "Lepton flavor non-conservation," *Progress in Particle and Nuclear Physics*, vol. 33, pp. 397–447, 1994.

[68] F. Deppisch, T. S. Kosmas, and J. W. F. Valle, "Enhanced μ^--e^- conversion in nuclei in the inverse seesaw model," *Nuclear Physics B*, vol. 752, no. 1-2, pp. 80–92, 2006.

[69] D. V. Forero, S. Morisi, M. Tortola, and J. W. F. Valle, "Lepton flavor violation and non-unitary lepton mixing in low-scale

type-I seesaw," *Journal of High Energy Physics*, vol. 2011, article 142, 2011.

[70] S. P. Das, F. F. Deppisch, O. Kittel, and J. W. F. Valle, "Heavy neutrinos and lepton flavor violation in left-right symmetric models at the LHC," *Physical Review D*, vol. 86, no. 5, Article ID 055006, 20 pages, 2012.

[71] A. A. Petrov and D. V. Zhuridov, "Lepton flavor-violating transitions in effective field theory and gluonic operators," *Physical Review D*, vol. 89, Article ID 033005, 2014.

[72] P. S. Amanik and G. M. Fuller, "Stellar collapse dynamics with neutrino flavor changing neutral currents," *Physical Review D*, vol. 75, Article ID 083008, 2007.

[73] J. Barranco, O. G. Miranda, C. A. Moura, and J. W. F. Valle, "Constraining nonstandard interactions in νee or $\nu\bar{e}$e scattering," *Physical Review D: Particles, Fields, Gravitation and Cosmology*, vol. 73, no. 11, Article ID 113001, 2006.

[74] O. G. Miranda, M. A. Tortola, and J. W. F. Valle, "Are solar neutrino oscillations robust?" *Journal of High Energy Physics*, vol. 2006, no. 10, article 8, 2006.

[75] J. Barranco, O. G. Miranda, and T. I. Rashba, "Sensitivity of low energy neutrino experiments to physics beyond the standard model," *Physical Review D*, vol. 76, Article ID 073008, 2007.

[76] T. S. Kosmas and J. D. Vergados, "Nuclear matrix elements for the coherent μ-e conversion process," *Physics Letters B*, vol. 215, no. 3, pp. 460–464, 1988.

[77] T. S. Kosmas and J. D. Vergados, "Study of the flavour violating (μ^-, e^-) conversion in nuclei," *Nuclear Physics A*, vol. 510, no. 4, pp. 641–670, 1990.

[78] T. S. Kosmas, J. D. Vergados, O. Civitarese, and A. Faessler, "Study of the muon number violating (μ^-, e^- conversion in a nucleus by using quasi-particle RPA," *Nuclear Physics Section A*, vol. 570, no. 3-4, pp. 637–656, 1994.

[79] T. S. Kosmas, S. Kovalenko, and I. Schmidt, "Nuclear $\mu^- - e^-$ conversion in strange quark sea," *Physics Letters B*, vol. 511, no. 2–4, pp. 203–208, 2001.

[80] T. S. Kosmas, S. Kovalenko, and I. Schmidt, "b-quark mediated neutrinoless μ^-–e^- conversion in presence of R-parity violation," *Physics Letters B*, vol. 519, no. 1-2, pp. 78–82, 2001.

[81] V. C. Chasioti and T. S. Kosmas, "A unified formalism for the basic nuclear matrix elements in semi-leptonic processes," *Nuclear Physics A*, vol. 829, no. 3-4, pp. 234–252, 2009.

[82] V. Tsakstara and T. S. Kosmas, "Low-energy neutral-current neutrino scattering on ^{128,130}Te isotopes," *Physical Review C*, vol. 83, Article ID 054612, 2011.

[83] V. Tsakstara and T. S. Kosmas, "Analyzing astrophysical neutrino signals using realistic nuclear structure calculations and the convolution procedure," *Physical Review C*, vol. 84, no. 6, Article ID 064620, 14 pages, 2011.

[84] H. de Vries, C. W. de Jager, and C. de Vries, "Nuclear charge-density-distribution parameters from elastic electron scattering," *Atomic Data and Nuclear Data Tables*, vol. 36, no. 3, pp. 495–536, 1987.

[85] T. W. Donnelly and J. D. Walecka, "Semi-leptonic weak and electromagnetic interactions with nuclei: isoelastic processes," *Nuclear Physics, Section A*, vol. 274, no. 3-4, pp. 368–412, 1976.

[86] W. M. Alberico, S. M. Bilenky, C. Giunti, and K. M. Graczyk, "Electromagnetic form factors of the nucleon: new fit and analysis of uncertainties," *Physical Review C*, vol. 79, no. 6, Article ID 065204, 12 pages, 2009.

[87] T. S. Kosmas and J. D. Vergados, "Nuclear densities with fractional occupation probabilities of the states," *Nuclear Physics A*, vol. 536, no. 1, pp. 72–86, 1992.

[88] J. Engel, "Nuclear form factors for the scattering of weakly interacting massive particles," *Physics Letters B*, vol. 264, pp. 114–119, 1991.

[89] P. Wintz, in *Proceedings of the First International Symposium on Lepton and Baryon Number Violation*, H. V. Klapdor-Kleingrothaus and I. V. Krivosheina, Eds., p. 534, Institute of Physics Publishing, Philadelphia, Pa, USA, 1998.